Flow and Displacement of Bingham Non-Newtonian Fluids in Porous Media

Y-S. Wu,* SPE, **Karsten Pruess,** and **P.A. Witherspoon,** Lawrence Berkeley Laboratory

Summary. This work presents a theoretical study of the flow and displacement of a Bingham fluid in porous media. An integral method of analyzing the single-phase flow of this type of fluid is developed. The accuracy of a newly developed approximate analytical solution for transient-flow problems is confirmed by comparison with numerical solutions. The flow behavior of a slightly compressible Bingham fluid is discussed, and a new well-test-analysis method is developed by use of the integral solution. To obtain some understanding of the physics of immiscible displacement with Bingham fluids, a Buckley-Leverett analytical solution with a practical graphic evaluation method was developed and applied to the problem of displacing a Bingham fluid with water. Results revealed that the saturation profile and displacement efficiency are controlled not only by the relative permeabilities, as in the case of Newtonian fluids, but also by the inherent complexities of Bingham non-Newtonian behavior. In particular, we found that in the displacement process with a Bingham fluid, a limiting maximum saturation exists beyond which no further displacement can be achieved.

Introduction

Flow of non-Newtonian fluids through porous media is encountered in many subsurface systems involving underground natural resource recovery or storage projects. In the past 30 years, a tremendous effort has been expended in developing quantitative analysis of flow of non-Newtonian fluids through porous media. Considerable progress has been reported, and much information is available in the chemical engineering, rheology, and petroleum engineering literature.[1-5] The theoretical investigations carried out in this field have concentrated mainly on single-phase power-law non-Newtonian fluid flow, while the experimental studies have intended to provide rheological models for non-Newtonian fluids and porous materials of interest.

Considerable evidence from laboratory experiments and field tests indicates that certain fluids exhibit a Bingham-type non-Newtonian behavior in porous media.[6,7] In these cases, flow takes place only after the applied pressure gradient exceeds a certain minimum value called the threshold pressure gradient. The flow of oil in many heavy-oil reservoirs does not follow Darcy's law but may be approximated by a Bingham fluid.[8]

The flow of foam in porous media is a focus of current research in many fields. Foam has been shown to be one of the most promising fluids for mobility control in underground energy recovery or storage projects. On a macroscopic scale, flow behavior of foam in porous media is non-Newtonian. The "power law" is generally used to correlate the apparent viscosities of foam with other flow properties for a given porous medium and surfactant.[9,10] It also has been observed experimentally that foam will start to flow in a porous medium only after the applied pressure gradient exceeds a certain threshold value.[11,12]

At present, there is no standard reliable approach in the petroleum engineering or groundwater literature to analyze well-test data for Bingham-fluid production or injection. Interpretation of transient-pressure responses of Bingham flow in porous media will be very important for heavy-oil development and for flow analysis of foam in porous media. The immiscible displacement of non-Newtonian and Newtonian fluids occurs in many EOR processes involving the injection of non-Newtonian fluids, such as polymer and foam solutions, or heavy-oil production by waterflooding. Very little research has been published, however, on multiphase flow of non-Newtonian and Newtonian fluids through porous media. Even with numerical methods, very few studies have examined the physics of displacement.[13] Therefore, the mechanisms of immiscible displacement involving non-Newtonian fluids in porous media are still not well-understood compared with those for Newtonian fluid displacement.

This paper presents a new method to analyze the transient flow of Bingham fluids through porous media, including an integral analysis method for single-phase flow and a Buckley-Leverett analytical solution for two-phase immiscible displacement with Bingham non-Newtonian fluids. To apply the theory to field problems, a new well-test-analysis method was developed, and its application demonstrated by analyzing two simulated pressure-drawdown and -buildup tests of a Bingham fluid. The displacement of a Bingham fluid by a Newtonian fluid is shown to proceed with rather limited efficiency owing to the presence of an ultimate (limited) displacement saturation, which is a characteristic of two-phase Bingham flow. Once the saturation in the two-phase flow system reaches the ultimate saturation, no further improvement of displacement efficiency can be obtained regardless of how long the displacement operation continues under the same flow conditions.

We also developed a numerical model for single- and multiphase Bingham-fluid flow through porous media by suitably modifying a general-purpose multiphase reservoir simulator. The model was used to test our analytical solutions and to generate well-testing data for the proposed well-test analysis for Bingham fluids.

Bingham Fluid and Rheological Model

As a special kind of non-Newtonian fluid, Bingham fluids (or plastics) exhibit a finite yield stress at zero shear rate. The physical behavior of fluids with a yield stress usually is explained as an internal structure in three dimensions that is capable of preventing movement for values of shear stress less than the yield value, τ_y. For shear stress $\tau > \tau_y$, the internal structure collapses completely, allowing shearing movement to occur. The characteristics of these fluids are defined by two constants: the yield stress, τ_y, which is the stress that must be exceeded for flow to begin, and the Bingham plastic coefficient, μ_B. The rheological equation for a Bingham plastic is[14]

$$\tau = \tau_y - \mu_B \dot{\gamma} \qquad (1)$$

The Bingham plastic concept has been found to approximate closely many real fluids existing in porous media, such as tarry and paraffin oils[7,8] and drilling muds and fracturing fluids,[15] which are suspensions of finely divided solids in liquids.

For a phenomenological description of flow in porous media, some equivalent or apparent viscosities for non-Newtonian fluid flow are needed in Darcy's equation. Therefore, many experimental and theoretical studies have investigated rheological models or correlations of apparent viscosities and flow properties for a given non-Newtonian fluid and porous material. For flow problems in porous media involving non-Newtonian Bingham fluids, the formulation of Darcy's law has been modified[6,7,16] to

$$\vec{u} = -\frac{k}{\mu_B}\left(1 - \frac{G}{|\nabla p|}\right)\nabla p \qquad (2a)$$

for $|\nabla p| > G$ and

$$\vec{u} = 0 \qquad (2b)$$

for $|\nabla p| \le G$. The physical meaning of the minimum pressure gradient, G, can be elucidated by considering flow of a Bingham fluid through a capillary with radius r. The Bingham flow equation was

*Now at HydroGeoLogic Inc.

TABLE 1—PARAMETERS FOR SINGLE-PHASE BINGHAM-FLUID FLOW

Initial pressure, p_i, Pa	10^7
Initial porosity, ϕ_i	0.20
Initial fluid density, ρ_i, kg/m^3	975.9
Formation thickness, h, m	1
Fluid viscosity, μ_{Ne}, Pa·s	0.35132×10^{-3}
Bingham coefficient, μ_B, Pa·s	5×10^{-3}
Fluid compressibility, c_f, Pa^{-1}	4.557×10^{-10}
Rock compressibility, c_r, Pa^{-1}	5×10^{-9}
Mass injection rate, q_m, kg/s	1
Permeability, k, darcies	1.0
Wellbore radius, r_w, m	0.1
Minimum pressure gradient, G, Pa/m	0, 10^2, 10^3, and 10^4

solved by Buckingham[17] to give the average flow velocity over the cross section of the tube. By comparing this velocity with Darcy's law, we obtain

$$G=\tau_y/(3r_t/8)=\tau_y/d. \quad \ldots\ldots (3)$$

Therefore, physically, G is the pressure gradient corresponding to the yield stress, τ_y, in a porous medium.

The two Bingham-fluid parameters, G and μ_B, should be determined by laboratory experiments or well tests for a porous medium flow problem. The range of values for G is quite large for different reservoirs. A reasonable value of G is on the order of 10^4 Pa/m for heavy oil,[8] and it may exceed 3.0×10^5 Pa/m for groundwater flow in certain clayey soils.[6]

Integral Analysis of Single-Phase Bingham Flow

The integral method has been widely used in the study of unsteady heat-transfer problems.[18] It is applied here to obtain an approximate analytical solution for Bingham-fluid flow in porous media. The integral approach to heat conduction uses a simple parametric representation of the temperature profile (e.g., by means of a polynomial) that is based on physical concepts, such as a time-dependent thermal-penetration distance. An approximate solution of the heat-transfer problem is then obtained from simple principles of heat-flux continuity and energy conservation. This solution satisfies the governing partial-differential equation only in an average, integral sense. It is encouraging to note, however, that many integral solutions to heat-transfer and fluid-mechanics problems have an accuracy that is generally acceptable for engineering applications.[18] When applied to fluid-flow problems in porous media, the integral method consists of assuming a pressure profile in the pressure-disturbance zone and determining the coefficients of the profile by use of the integral mass-balance equation.[19]

In analogy to the heat-conduction problem,[18,20] we first assumed a pressure profile of the form

$$p(r,t)-p_i=[p_n(r)]\ln(r),\ [r_w\le r\le r_w+\delta(t)], \quad \ldots\ldots (4)$$

where $p_n(r)$ is an nth-degree polynomial in r, and the time dependence is implicitly included in the coefficients of the polynomial, which is dependent on the pressure-penetration distance, $\delta(t)[p_n(\delta)=0]$. We found, however, that solutions in terms of profiles given by Eq. 4 are not accurate when compared with the Theis solution for the limiting case of a Newtonian fluid ($G=0$) and always introduce 5% to 10% errors. More accurate solutions were obtained for radial flow in a porous medium with pressure profiles of the form

$$p(r,t)-p_i=K\ln[p_n(r)], \quad \ldots\ldots (5)$$

where K is a constant.

Mathematical Formulation and Integral Solution. The problem considered here involves production of a Bingham fluid from a fully penetrating well in an infinite horizontal reservoir of constant thickness; the formation is saturated only with the Bingham fluid. The basic assumptions are (1) isothermal, isotropic, and homogeneous formation; (2) single-phase horizontal flow without gravity effects; (3) Darcy's law (Eq. 2) applies; and (4) constant fluid properties and formation permeability. The governing flow equation can be derived by combining the modified Darcy's law with the continuity equation and is expressed in a radial coordinate system as

$$\frac{k}{r}\frac{\partial}{\partial r}\left[\frac{\rho(p)}{\mu_B}r\left(\frac{\partial p}{\partial r}-G\right)\right]=\frac{\partial}{\partial t}[\rho(p)\phi(p)]. \quad \ldots\ldots (6)$$

The density of the Bingham fluid, $\rho(p)$, and the porosity of the formation, $\phi(p)$, are functions of pressure only.

The initial condition is

$$p(r,t=0)=p_i,\ r\ge r_w. \quad \ldots\ldots (7)$$

At the wellbore inner boundary, $r=r_w$, the fluid is produced at a given mass production rate, $q_m(t)$; i.e.,

$$\frac{2\pi r_w kh\rho(p_w)}{\mu_B}\left(\frac{\partial p}{\partial r}-G\right)_{r=r_w}=q_m(t), \quad \ldots\ldots (8)$$

where $p_w=p_w(t)=p(r_w,t)$, the wellbore pressure.

The integral solution for radial flow into a well under a specified mass production rate, $q_m(t)$, has been obtained with the pressure profile of Eq. 5 and an added inhomogeneous term as[19]

$$p(r,t)=p_i+(r-r_w\eta)G-\frac{q_m(t)\mu_B}{2\pi kh}\frac{1}{\rho(p_w)}\left[\frac{1+2\delta(t)/r_w}{2\delta(t)/r_w}\right]\times\ln\left[\frac{2r/r_w}{\eta}-\left(\frac{r/r_w}{\eta}\right)^2\right], \quad \ldots\ldots (9)$$

where $\eta=1+\delta(t)/r_w$. The unknowns, wellbore pressure, p_w, and pressure-penetration distance, $\delta(t)$, are determined by simultaneously solving Eq. 9 and the following integral equation:

$$\int_{r_w}^{r_w+\delta(t)}2\pi hr\rho(p)\phi(p)\mathrm{d}r=-\int_0^t q_m(t)\mathrm{d}t+\pi h\rho_i\phi_i\{[r_w+\delta(t)]^2-r_w^2\}, \quad \ldots\ldots (10)$$

where $\rho_i=\rho(p_i)$ and $\phi_i=\phi(p_i)$. Eq. 10 is simply a mass-balance equation in the pressure-disturbance region.

For slightly compressible flow, we obtain the following explicit expression of the integral mass-balance equation:

$$\int_0^t q_m(t)\mathrm{d}t+\rho_i\phi_i c_t r_w^2\left\{2\pi hr_w G\left(-\frac{1}{6}\eta^3+\frac{1}{2}\eta-\frac{1}{3}\right)+\frac{q_m(t)\mu_B}{k\rho(p_w)}\left[\frac{1+2\delta(t)/r_w}{2\delta(t)/r_w}\right]\left[-\frac{3}{2}\eta^2+\eta+\frac{1}{2}+2\eta\ln(\eta)-\frac{1}{2}[1-4\eta^2]\ln\left(\frac{2\eta-1}{\eta^2}\right)\right]\right\}=0. \quad \ldots\ldots (11)$$

Verification of Integral Solutions. The solution from the integral method is approximate and needs to be checked by comparison with an exact solution or with numerical results. For the special case of minimum pressure gradient, $G=0$, a Bingham fluid becomes Newtonian. Then, the Theis solution can be used to check the integral solution given by Eqs. 9 and 11. Many comparisons have been performed between the integral and Theis solutions with different fluid and formation properties, and excellent agreement has been obtained in all cases, with maximum errors in wellbore pressure values $<0.1\%$.

For the radial-flow problem of Bingham-fluid production with $G>0$, the results from the integral solution have been examined by comparison with numerical simulations (see the Appendix). Agreement between the approximate integral and numerical results was found to be excellent for the entire transient-flow period, with maximum errors no more than 0.1%.

Comparison of the integral solutions with both the exact Theis solution and the numerical simulation indicates that the pressure profile (Eq. 5) can accurately represent radial flow of both Newtonian and Bingham fluids.

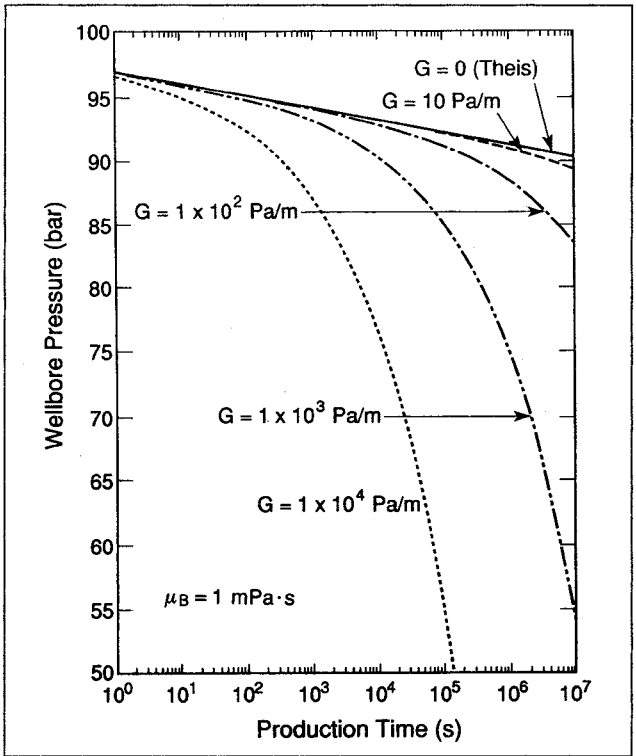

Fig. 1—Transient wellbore pressure during Bingham-fluid production calculated from the integral solution for different values of the minimum pressure gradient ($\rho_f = 1000$ kg/m^3, $c_t = 6.56 \times 10^{-10}$ Pa^{-1}, and $q_m = 0.5$ kg/s).

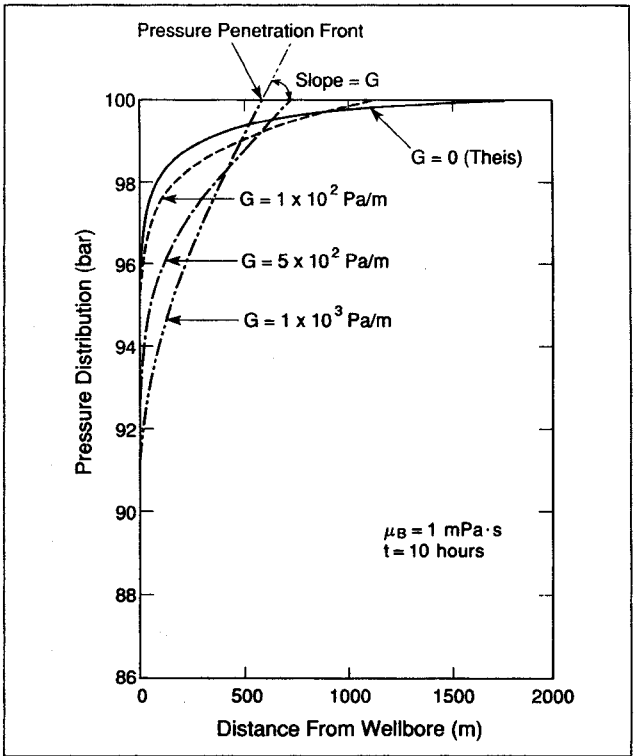

Fig. 2—Pressure distributions during Bingham-fluid production for different values of the minimum pressure gradient ($\rho_f = 1000$ kg/m^3, $c_t = 6.56 \times 10^{-10}$ Pa^{-1}, and $q_m = 0.5$ kg/s).

Effects of Minimum Pressure Gradient. We used the integral solution for the problem with the parameters specified in **Table 1** to examine flow behavior for a range of rheological parameters. **Fig. 1** shows pressure drawdown at the wellbore for a constant mass production rate. The flow resistance increases with an increase in G in a reservoir. Therefore, to maintain the same production rate, the wellbore pressure decreases more rapidly with increasing G, as indicated in Fig. 1. **Fig. 2** shows the pressure profiles after continuous production for 10 hours at different values of G. As the minimum pressure gradient increases, the pressure drops penetrate less deeply into the formation because of greater flow resistance.

Well-Testing Analysis of Bingham-Fluid Flow. An analysis method for transient-pressure tests during Bingham-fluid production or injection into a well can be developed on the basis of the integral and numerical solutions of this work. The most important parameters for Bingham-fluid flow through porous media are the two characteristic rheological parameters, the minimum pressure gradient, G, and the coefficient, μ_B. It is always possible to obtain these parameters by trial and error, using the integral and numerical solutions to match the observed pressure data. The following approach is more accurate and convenient to use, however, and is recommended for field applications.

Let us consider the pressure-buildup behavior in an infinite horizontal formation with a production well. After some period of production, the well is shut in. The pressure in the system will build up until a new equilibrium is achieved at a long enough shut-in period that theoretically is at infinite time. The pressure gradient everywhere in the pressure-penetration zone is expected to be equal to the minimum pressure gradient. This is confirmed by a numerical study of the pressure buildup after $t_p = 1{,}000$ seconds of Bingham-fluid production from a well, as shown in **Fig. 3**. If the cumulative mass production rate, q_c, before the well is shut in is known, the minimum pressure gradient of the system can be calculated from the observed stabilized wellbore pressure, p_w,[19] with

$$G = 1/2 q_c \left(\pi h r_w \rho_i \phi_i c_t (\Delta p)^2 + \{[\pi h r_w \rho_i \phi_i c_t (\Delta p)^2]^2 + 4\pi h \rho_i \phi_i c_t (\Delta p)^3/3\}^{1/2}\right), \quad \ldots\ldots\ldots\ldots\ldots\ldots\ldots\ldots (12)$$

where $\Delta p = p_i - p_w$. Note that the minimum pressure gradient determined by the pressure-buildup method given in Eq. 12 pertains to equilibrium in the system and is independent of flow properties, such as permeability k, and the coefficient μ_B.

To illustrate the procedure of calculating the value of G, a test example was created by numerical simulation. A Bingham fluid is produced at $q_m = 0.1$ kg/s until $t_p = 1{,}000$ seconds when the well is shut in. The stable wellbore pressure is found to be $p_w = 0.97474 \times 10^7$ Pa at a long shut-in time. Thus, the minimum pressure gradient can be calculated with Eq. 12:

$$G = \frac{1}{200} \times [1.1737423 \times 10^5 + (1.377671 \times 10^8 + 3.953165 \times 10^{12})^{1/2}]$$

$$= 10{,}000.14 \text{ Pa/m}. \quad \ldots\ldots\ldots\ldots\ldots\ldots\ldots\ldots\ldots\ldots\ldots\ldots (13)$$

This is very accurate compared with the input value, $G = 10{,}000$ Pa/m, in the numerical calculation. The pressure-penetration distance at equilibrium is

$$\delta(t) = \frac{\Delta p}{G} = \frac{2.526 \times 10^5}{10{,}000.14} = 25.26 \text{ m}. \quad \ldots\ldots\ldots\ldots\ldots\ldots\ldots\ldots (14)$$

Fig. 3 shows the pressure distribution after a long shut-in time calculated from the mass balance. The analytical and numerical results are essentially identical.

The apparent mobility, k/μ_B, is a flow property of the system and may be determined by transient-flow tests when G is not very large. **Fig. 4** shows that semilog straight lines occur in the pressure-drawdown curves during the early transient period; they are almost parallel to the straight line from the Theis solution ($G = 0$). Therefore, if the semilog straight line is developed during the early flow time in the transient pressure drawdown, the conventional analysis technique[21,22] can be used to estimate the value of k/μ_B for a Bingham fluid. For example, the slope m of the semilog straight-line

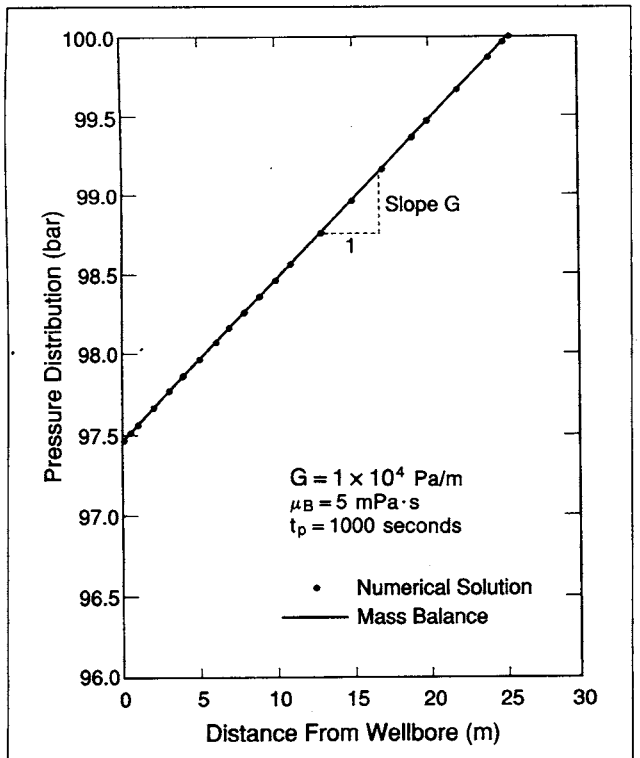

Fig. 3—Pressure distribution at long shut-in time following 1000 seconds of Bingham-fluid production ($\mu_B = 5 \times 10^{-3}$ Pa·s, $c_t = 9.0 \times 10^{-9}$ Pa^{-1}, and $q_m = 0.1$ kg/s).

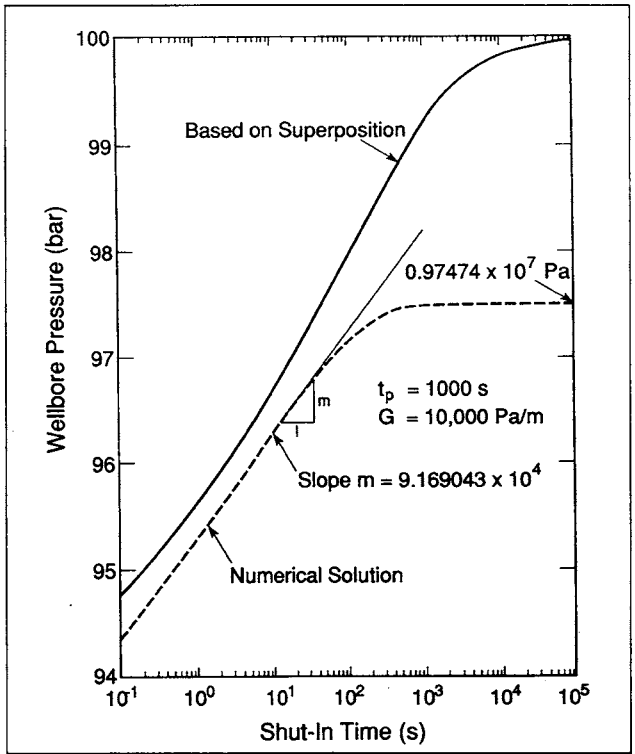

Fig. 4—Numerically simulated pressure buildup during well shut-in after 1000 seconds of Bingham-fluid production ($\mu_B = 5 \times 10^{-3}$ Pa·s, $c_t = 9.0 \times 10^{-9}$ Pa^{-1}, and $q_m = 0.1$ kg/s).

part of the curve $G=100$ Pa/m in Fig. 1 is measured as 9.23574×10^4 Pa/log$_{10}$ cycle. Then, k/μ_B can be estimated as

$$\frac{k}{\mu_B} = \frac{2.303 \times 0.5/1000.0}{4 \times 3.1415926 \times 1.0 \times 9.23574 \times 10^4}$$

$$= 9.92 \times 10^{-10} \text{ m}^2/\text{Pa·s}. \quad \ldots\ldots\ldots\ldots\ldots\ldots (15)$$

In the simulated test, the actual input is

$$\frac{k}{\mu_B} = \frac{0.9869 \times 10^{-12}}{1.0 \times 10^{-3}} = 9.87 \times 10^{-10} \text{ m}^2/\text{Pa·s}, \quad \ldots\ldots (16)$$

so the relative error is only 0.5%.

For a large G, semilog straight lines hardly exist in the pressure drawdowns. The pressure-buildup curves, however, result in a long straight line even for $G=10{,}000$ Pa/m (see Fig. 4). This pressure-buildup test is conducted by the numerical code. The top curve in Fig. 4 is the prediction from the integral solution based on the superposition principle. As expected, the superposition technique cannot be used for this nonlinear problem. The slope of the semilog straight line of Fig. 4 is measured as $m=9.169043 \times 10^4$ log$_{10}$ cycle, so we have

$$\frac{k}{\mu_B} = \frac{2.303 \times 0.1/975.9}{4 \times 3.1415926 \times 1.0 \times 9.169043 \times 10^4}$$

$$= 2.05 \times 10^{-10} \text{ m}^2/\text{Pa·s}. \quad \ldots\ldots\ldots\ldots\ldots\ldots (17)$$

This value differs by only 3.8% from the input value, $k/\mu_B = 1.97 \times 10^{-10}$ m^2/Pa·s.

If no straight lines are developed in either pressure-drawdown or -buildup curves, then the apparent mobility can be obtained by matching the observed transient-pressure data with the integral solution. G should always be calculated first from the mass balance (Eq. 12), which is always applicable. The only remaining unknown is the apparent mobility, k/μ_B, which can be determined easily by trial and error with the integral solution.

TABLE 2—PARAMETERS FOR LINEAR BINGHAM-FLUID DISPLACEMENT

Porosity, ϕ	0.20
Permeability, k, darcies	1
Cross-sectional area, A, m^2	1
Injection rate, i, m^3/s	1.0×10^{-6}
Injection time, t, hours	10
Displacing Newtonian viscosity, μ_{Ne}, mPa·s	1
Irreducible saturation, S_{nNir}	0.20
Bingham plastic coefficient, μ_B, mPa·s	4.0
Minimum pressure gradient, G, Pa/m	10 000

Immiscible Displacement of a Bingham Non-Newtonian Fluid by a Newtonian Fluid

In an effort to obtain some insight into the physics behind two-phase immiscible displacement with non-Newtonian fluids, we developed a Buckley-Leverett analytical solution for 1D flow in porous media.[23] Here, this analytical solution is used to study the displacement of a Bingham non-Newtonian fluid by a Newtonian fluid. One possible application of this study is the production of heavy oil by waterflooding. Note that because of the 1D approximation in our analysis, we cannot address issues of viscous or gravitational instabilities.

Analytical Solution for Bingham-Fluid Displacement. The analytical solution obtained for immiscible non-Newtonian fluid displacement[23] is in the same form as the Buckley-Leverett[24] frontal-advance equation. The crucial difference is in the fractional-flow function, which now depends, not only on relative permeability data, but also, through apparent or effective viscosities, on the rheological properties of the non-Newtonian fluid. This feature introduces a strong rate dependence into the displacement process, as will be seen below. The fractional-flow function of the

displacing Newtonian fluid is defined as the ratio of the flow rate of the Newtonian fluid and the total rate, and is given by[25]

$$f_{Ne}=\frac{1}{1+\left[\frac{k_{rnN}(S_{Ne})}{k_{rNe}(S_{Ne})}\right]\left(\frac{\mu_{Ne}}{\mu_{nN}}\right)}$$

$$+\frac{\frac{Akk_{rnN}(S_{Ne})}{\mu_{nN}q(t)}(\rho_{nN}-\rho_{Ne})g\sin\alpha}{1+\left[\frac{k_{rnN}(S_{Ne})}{k_{rNe}(S_{Ne})}\right]\left(\frac{\mu_{Ne}}{\mu_{nN}}\right)}, \quad \ldots\ldots\ldots\ldots (18)$$

where μ_{nN} is a function of saturation and flow potential gradient:

$$\mu_{nN}=\mu_{nN}(\nabla\Phi,S_{Ne}). \quad \ldots\ldots\ldots\ldots (19)$$

Introducing coordinates such that flow takes place in the x direction, the potential gradient component in the x direction is

$$\partial\Phi/\partial x=(\partial p/\partial x)+\rho_{nN}g\sin\alpha. \quad \ldots\ldots\ldots\ldots (20)$$

Eqs. 18 and 19 indicate that the fractional flow of the displacing Newtonian phase, f_{Ne}, is generally a function of both saturation and potential gradient. Under the usual simplifications made in the Buckley-Leverett problem (incompressible 1D linear flow and uniform fluid and formation properties), however, the potential gradient is related uniquely to saturation as follows[23]:

$$i(t)+Ak\left[\frac{k_{rNe}(S_{nN})}{\mu_{Ne}}+\frac{k_{rnN}(S_{nN})}{\mu_{nN}(\partial\Phi/\partial x,S_{nN})}\right]\frac{\partial p}{\partial x}$$

$$+k\left[\frac{\rho_{Ne}k_{rNe}(S_{nN})}{\mu_{Ne}}+\frac{\rho_{nN}k_{rnN}(S_{nN})}{\mu_{nN}(\partial\Phi/\partial x,S_{nN})}\right]g\sin\alpha=0. \quad \ldots\ldots (21)$$

Therefore, the fractional-flow function in Eq. 18 ends up being a function of saturation only, and the Welge[26] graphic method can be applied for evaluation of non-Newtonian fluid displacement.[23] The rheological model for the apparent viscosity of a Bingham plastic fluid can be obtained from Eq. 2:

$$\mu_{nN}=\mu_B/[1-(G/|\partial\Phi/\partial x|)] \quad \ldots\ldots\ldots\ldots (22a)$$

for $|\partial\Phi/\partial x|>G$, and

$$\mu_{nN}=\infty \quad \ldots\ldots\ldots\ldots (22b)$$

for $|\partial\Phi/\partial x|\le G$. For a particular saturation of the Newtonian phase, S_{Ne}, the corresponding flow potential gradient for the non-Newtonian phase can be derived by introducing Eq. 22a into Eq. 21 as follows:

$$-(\partial\Phi/\partial x)_{S_{Ne}}=-\rho_{nN}\,g\sin\alpha+$$

$$\frac{\frac{i}{Ak}+\frac{k_{rnN}(S_{Ne})}{\mu_B}G+\frac{k_{rNe}(S_{Ne})}{\mu_{Ne}}\rho_{Ne}g\sin\alpha+\frac{k_{rnN}(S_{Ne})}{\mu_B}\rho_{nN}g\sin\alpha}{\frac{k_{rnNe}(S_{Ne})}{\mu_{Ne}}+\frac{k_{rnN}(S_{Ne})}{\mu_B}}$$

$$\ldots\ldots\ldots\ldots (23)$$

The apparent viscosity for the Bingham fluid is determined by use of Eq. 23 in Eq. 22, and then the fractional-flow curve is calculated from Eq. 18.

Displacement of a Bingham Non-Newtonian Fluid by a Newtonian Fluid. Initially, the system is assumed to be saturated with only a Bingham fluid, and a Newtonian fluid is injected at a constant volumetric rate at the inlet, $x=0$, starting from $t=0$. The relative permeabilities are given as functions of saturation of the displacing Newtonian fluid according to the analytical correlation by Willhite[25]:

$$k_{r_{nN}}=0.75(1-S_D)^2 \quad \ldots\ldots\ldots\ldots (24)$$

and $k_{r_{Ne}}=0.75(S_D)^2$, $\ldots\ldots\ldots\ldots (25)$

with $S_D=S_{Ne}/(1-S_{nNir})$. **Table 2** summarizes the fluid and rock properties.

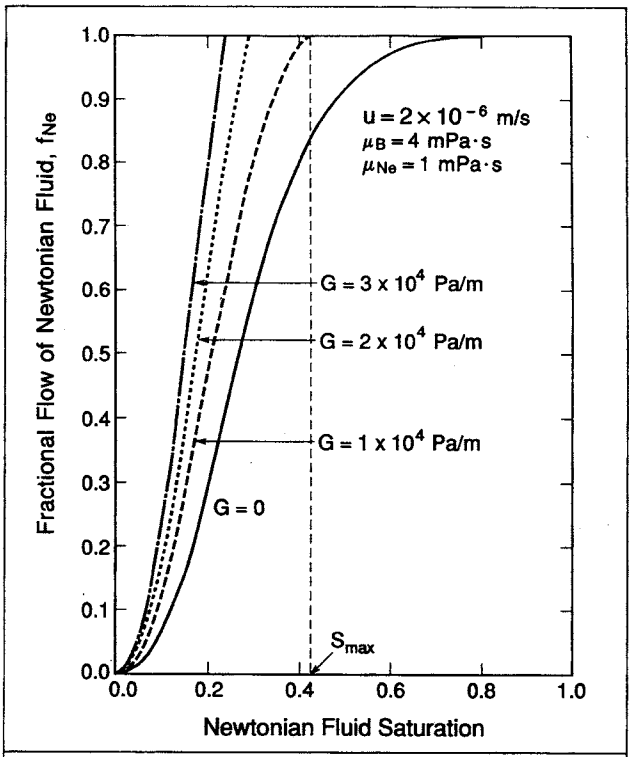

Fig. 5—Fractional-flow curves for a Bingham fluid displaced by a Newtonian fluid for different minimum pressure gradients.

Effects of Non-Newtonian Rheological Properties. A basic feature of the displacement process of a Bingham fluid in porous media is the existence of an ultimate or maximum displacement saturation, S_{max}, for the displacing Newtonian phase (see **Figs. 5 and 6**). The maximum displacement saturation occurs at the point of the fractional-flow curve where $f_{Ne}=1.0$. For this particular displacement system, initially saturated with only the Bingham fluid, the displacing saturation cannot exceed the maximum value S_{max}. The resulting saturation distributions are given in Fig. 6 for different G. It is obvious that the sweep efficiency (defined as the ratio of displacing Newtonian fluid volume and in-situ Bingham fluid volume) decreases rapidly as G increases. In contrast, for Newtonian displacement, the ultimate saturation of the displacing fluid is equal to the total mobile saturation of the displacing fluid, as shown by the curve for $G=0$ in Fig. 6.

Physically, the phenomenon of ultimate displacement saturation occurs as the flow potential gradient approaches the minimum threshold pressure gradient, G, at which the apparent viscosity is infinite. Then the only flowing phase is the displacing Newtonian fluid. Consequently, once the maximum saturation is reached for a flow system, no improvement of sweep efficiency can be obtained no matter how long the displacement process continues, as shown in Fig. 6. The flow condition in reservoirs is more complicated than in this linear semi-infinite system. Because oil wells usually are drilled according to certain patterns, some regions always exist with low potential gradients between production and injection wells. The presence of the ultimate displacement saturation for a Bingham fluid indicates that no oil can be driven out of these regions. Therefore, the ultimate displacement saturation phenomenon will contribute to the low oil recovery observed in heavy-oil reservoirs developed by waterflooding, in addition to effects from the high oil viscosity.

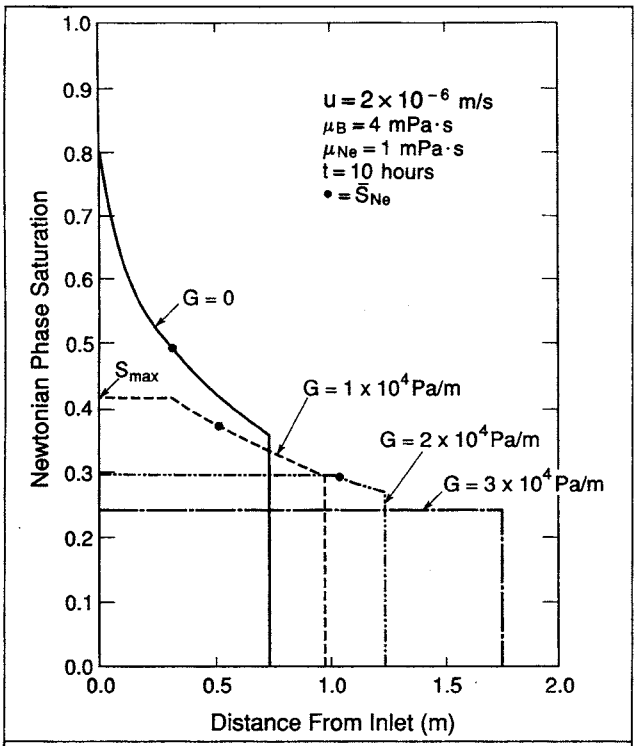

Fig. 6—Newtonian phase saturation distributions, for different values of the minimum pressure gradient of a Bingham fluid.

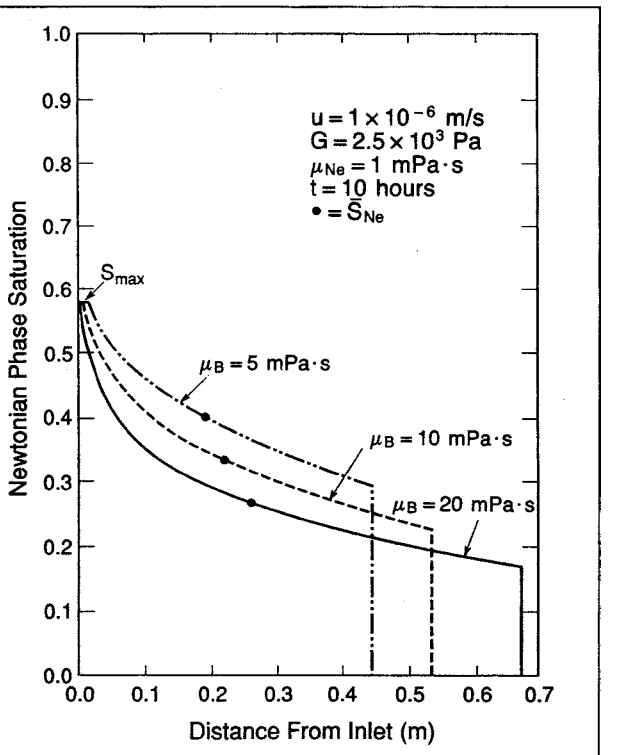

Fig. 7—Newtonian phase saturation distributions for different values of the Bingham coefficient, μ_B.

Fig. 7 shows the effects of the other rheological parameter, the Bingham plastic coefficient μ_B. Note that the ultimate displacement saturations change little with μ_B. The average saturations in the swept zones, however, are quite different for different values of μ_B. The ultimate displacement saturation is essentially determined by G. Changes in μ_B have little effect on the ultimate displacement saturation because the flow potential gradient in Eq. 23 hardly varies with μ_B as $\partial p/\partial x \rightarrow G$.

Effects of Injection Rate. In this problem, a Bingham fluid in a horizontal porous medium is displaced by water. If the water injection rate at the inlet is increased, the pressure gradient in the system will increase and the apparent viscosity for the displaced Bingham fluid will be reduced. Therefore, a better sweep efficiency will result. **Fig. 8** presents the saturation profiles after 10 hours of injection at the different rates. Note that both the sweep efficiency and the ultimate displacement saturation can be increased greatly by increasing the injection rate.

Effects of Gravity. The effects of gravity on Bingham-fluid displacement by a Newtonian fluid can be examined by considering the following example. A heavier Newtonian fluid with $\rho_{Ne} =$ 1,000 kg/m is used to displace a Bingham fluid with $\rho_{nN} = 850$ kg/m. The flow directions are upward ($\alpha = \pi/2$), horizontal ($\alpha = 0$), and downward ($\alpha = -\pi/2$). Even though displacement flow directions in oil reservoirs are mostly horizontal, upward or downward flow may occur because of the inhomogeneity of layered formations or may occur in laboratory displacement tests. **Fig. 9** shows the saturation distributions after 10 hours of displacement. The difference in density of the two fluids is small, so the influence of gravity on displacement efficiency near the front is not very significant. However, gravity does change the ultimate displacement saturation. The best displacement performance is obtained by upward flow. Because gravity resists the upward flow of the heavier displacing phase, the flow potential gradient must be larger to maintain the same flow rate. Consequently, the apparent viscosity of the Bingham fluid is decreased for upward flow, resulting in better sweep efficiency.

Conclusions

An approximate integral solution was obtained for the problem of Bingham flow through porous media. Its accuracy was confirmed by comparison with exact and numerical solutions. Our analytical and numerical studies show that the transient-flow behavior of slightly compressible Bingham fluids is essentially controlled by the non-Newtonian properties: the minimum pressure gradient, G, and the Bingham plastic coefficient, μ_B. Therefore, transient pressure data can provide important information related to non-Newtonian fluid and formation properties. A well-test-analysis technique developed in this study uses flow-test data to estimate non-Newtonian flow properties.

The integral method with a new pressure profile developed in this work is applicable to more general radial-flow problems in porous media. It is especially useful when the flow equation is nonlinear and other analytical approaches cannot apply.

The fundamental feature of immiscible displacement involving a Bingham plastic fluid is that an ultimate displacement saturation exists that is essentially determined by the minimum pressure gradient, G. This saturation can be considerably larger than residual saturations from relative permeability effects. Once the saturation approaches the ultimate saturation in the formation, no further displacement can be obtained regardless of how long the displacement lasts for a given operating condition. A simple way to gain a better sweep efficiency is to increase injection rates, thereby reducing the apparent viscosity of the displaced Bingham fluid. A better displacement also can be obtained by using gravity to increase the flow potential gradient in the flow direction for a given flow rate.

Nomenclature

A = cross-sectional area, m^2
c_f = fluid compressibility, Pa^{-1}
c_r = formation compressibility, Pa^{-1}
c_t = total compressibility, Pa^{-1}
d = characteristic pore size of porous medium, $3r_t/8$, m
f_{Ne} = fractional flow of Newtonian phase
f_{nN} = fractional flow of non-Newtonian phase
g = magnitude of gravitational acceleration, m/s^2
G = minimum pressure gradient, Pa/m
h = formation thickness, m
$i(t)$ = volumetric injection rate, m^3/s
k = absolute permeability, m^2

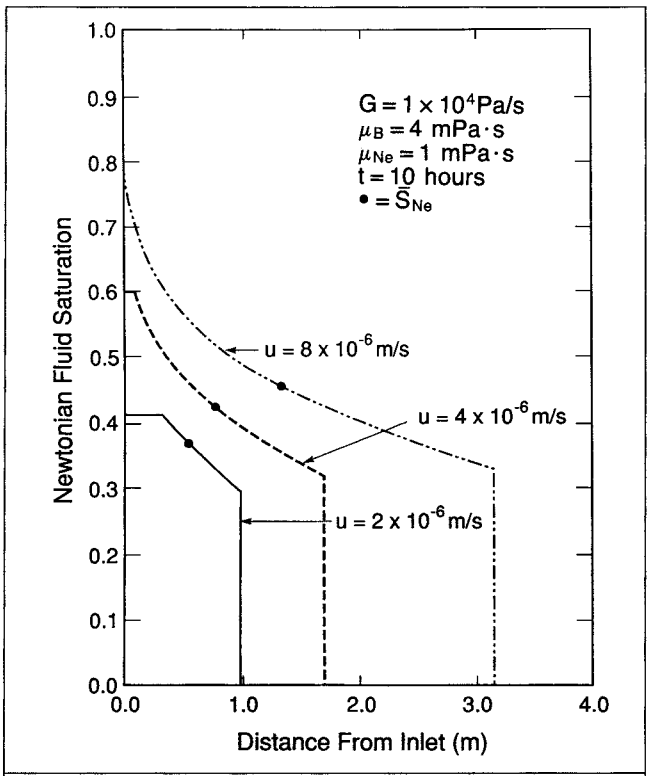

Fig. 8—Newtonian phase saturation distributions for different injection rates of a Newtonian fluid displacing a Bingham fluid.

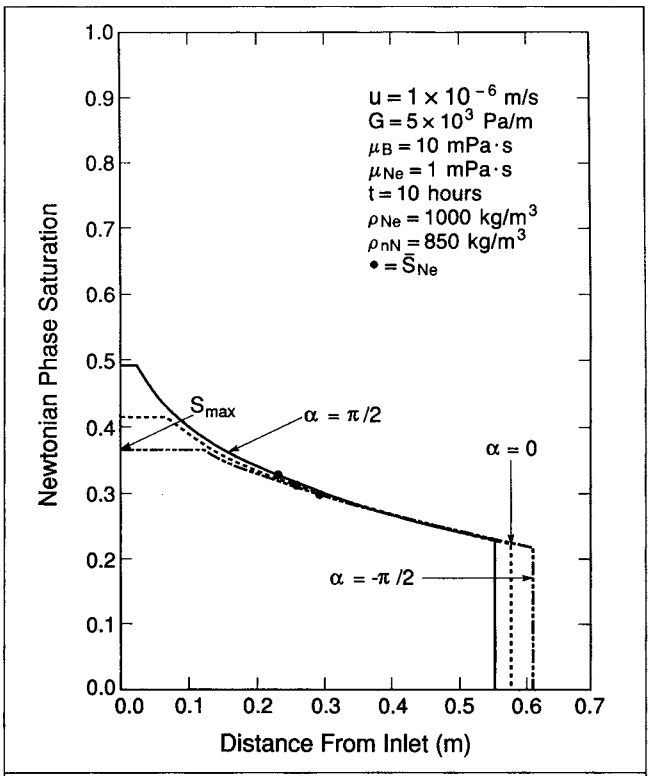

Fig. 9—Newtonian phase saturation distributions for Bingham-fluid displacement by a Newtonian fluid with gravity effects.

$k_{r\mathrm{Ne}}$ = relative permeability to Newtonian phase
$k_{r\mathrm{nN}}$ = relative permeability to non-Newtonian phase
K = constant
m = slope of semilog curves, Pa/log-cycle
n_c = number of fluid components
n_P = number of fluid phases
p = pressure, Pa
p_i = initial formation pressure, Pa
$p_n(r)$ = nth-degree polynomial in r
p_w = wellbore flowing pressure, Pa
∇p = pressure gradient, Pa/m
q = volumetric production rate, m^3/s
q_c = cumulative mass production, kg
$q_m(t)$ = mass production rate, kg/s
r = radial distance coordinate, m
r_t = tube radius, m
r_w = wellbore radius, m
S = saturation
$S_{\max}$ = ultimate displacement saturation
S_{Ne} = Newtonian phase saturation
$\bar{S}_{\mathrm{Ne}}$ = average Newtonian phase saturation
S_{nN} = non-Newtonian phase saturation
S_{nNir} = irreducible non-Newtonian phase saturation
t = time, seconds
t_p = production time, seconds
u = Darcy velocity, m/s
$\vec{u}$ = Darcy velocity vector, m/s
x = distance from inlet coordinate, m
α = angle between flow direction and horizontal plane
$\dot{\gamma}$ = shear rate, $\mathrm{seconds}^{-1}$
$\delta(t)$ = pressure-penetration distance, m
η = $1+\delta(t)/r_w$
μ_{B} = Bingham plastic coefficient, Pa·s
μ_{Ne} = Newtonian viscosity, Pa·s
μ_{nN} = non-Newtonian apparent viscosity, Pa·s
ρ = fluid density, kg/m^3
ρ_{Ne} = density of Newtonian fluid, kg/m^3
ρ_{nN} = density of non-Newtonian fluid, kg/m^3
τ = shear stress, Pa
τ_y = yield stress, Pa
ϕ = porosity
ϕ_i = initial formation porosity
Φ = flow potential, Pa
$\nabla\Phi$ = flow potential gradient, Pa/m
$\nabla\Phi_e$ = effective flow potential gradient, Pa/m

Subscripts

B = Bingham fluid
D = dimensionless
e = equivalent
i = initial
m = mass
n = nth degree
Ne = Newtonian fluid
nN = non-Newtonian fluid
rNe = relative to Newtonian fluid
rnN = relative to non-Newtonian fluid
t = total
w = wellbore
y = yield

Acknowledgments

We are grateful to R.W. Zimmerman and M. Ripperda for critical review of the manuscript. This work was supported by the Office of Basic Sciences, U.S. DOE, under Contract No. DE-AC03-76SF00098.

References

1. Savins, J.G.: "Non-Newtonian Flow Through Porous Media," *Ind. & Eng. Chem.* (1969) **61,** 18-47.
2. Gogarty, W.B.: "Rheological Properties of Pseudoplastic Fluids in Porous Media," *SPEJ* (June 1967) 149-59; *Trans.*, AIME, **240.**
3. van Poollen, H.K. and Jargon, J.R.: "Steady-State and Unsteady-State Flow of Non-Newtonian Fluids Through Porous Media," *SPEJ* (March 1969) 80-88; *Trans.*, AIME, **246.**
4. Ikoku, C.U. and Ramey, H.J. Jr.: "Transient Flow of Non-Newtonian Power-Law Fluids in Porous Media," *SPEJ* (June 1979) 164-74.
5. Odeh, A.S. and Yang, H.T.: "Flow of Non-Newtonian Power-Law Fluids Through Porous Media," *SPEJ* (June 1979) 155-63.

Authors

Wu Pruess Witherspoon

Yu-Shu Wu is a research hydrogeologist for HydroGeoLogic Inc. in Herndon, VA. His research interests are reservoir simulation methods and multiphase flow phenomena in permeable media for EOR. He holds a BS degree in petroleum engineering from Daqing Petroleum Inst., an MS degree in petroleum engineering from Southwest Petroleum Inst., China, and a PhD in groundwater hydrogeology from the U. of California, Berkeley. Karsten Pruess is a senior scientist in Lawrence Berkeley Laboratory's Earth Sciences Div., where he researches the modeling of subsurface flow systems. He previously was a researcher and lecturer at the U. of Bremen and the U. of Frankfurt, Germany. He holds a PhD degree in physics from the U. of Frankfurt. Pruess was a member of the 1985–87 Editorial Review Committee and the program committee for the 1991 Reservoir Simulation Symposium. Paul A. Witherspoon is professor emeritus of geological engineering at the U. of California, Berkeley, and faculty senior scientist at the Lawrence Berkeley Laboratory. He holds BS and MS degrees in petroleum engineering and a PhD degree in geology from the U. of Illinois. His research interests are in fluid flow through porous and fractured rocks.

6. Bear, J.: *Dynamics of Fluids in Porous Media,* Elsevier Science Publishers, New York City (1972).
7. Barenblatt, G.E., Entov, B.M., and Rizhik, B.M.: *Flow of Liquids and Gases in Natural Formations,* Nedra, Moscow (1984).
8. Mirzadjanzade, A.KH. *et al.*: "On the Special Features of Oil and Gas Field Development Due to Effects of Initial Pressure Gradient," *Proc.*, 8th World Pet. Cong., Special Papers, Elsevier Science Publishers, London (1971).
9. Patton, J.T., Holbrook, S.T., and Hsu, W.: "Rheology of Mobility-Control Foams," *SPEJ* (June 1983) 456–60.
10. Hirasaki, G.J. and Lawson, J.B.: "Mechanisms of Foam Flow in Porous Media: Apparent Viscosity in Smooth Capillaries," *SPEJ* (April 1985) 176–90.
11. Albrecht, R.A. and Marsden, S.S.: "Foams as Blocking Agents in Porous Media," *SPEJ* (March 1970) 51–55.
12. Witherspoon, P.A. *et al.*: "Feasibility Analysis and Development of Foam Protected Underground Natural Gas Storage Facilities," final report, Earch Sciences Div., Lawrence Berkeley Laboratory, Berkeley, CA (1989).
13. Gencer, C.S. and Ikoku, C.U.: "Well Test Analysis for Two-Phase Flow of Non-Newtonian Power-Law and Newtonian Fluids," *ASME J. Energy Resources Tech.* (1984) 295–304.
14. Bird, R.B., Stewart, W.E., and Lightfoot, E.N.: *Transport Phenomena,* John Wiley & Sons Inc., New York City (1960).
15. Hughes, W.F. and Brighton, J.A.: *Theory and Problems of Fluid Dynamics,* Schaum's Outline Series, McGraw-Hill Book Co., New York City (1967) 230–41.
16. Scheidegger, A.E.: *The Physics of Flow Through Porous Media,* U. of Toronto Press, Toronto (1974).
17. Skelland, A.H.P.: *Non-Newtonian Flow and Heat Transfer,* John Wiley & Sons Inc., New York City (1967).
18. Ozisik, M.N.: *Heat Conduction,* John Wiley & Sons Inc., New York City (1980).
19. Wu, Y-S. "Theoretical Studies of Non-Newtonian and Newtonian Fluid Flow Through Porous Media," PhD dissertation, U. of California, Berkeley (1990).
20. Lardner, T.J. and Pohle, F.V.: "Application of the Heat Balance Integral to Problems of Cylindrical Geometry," *J. Appl. Mech.* (1961) 310–12.
21. Earlougher, R.C. Jr.: *Advances in Well Test Analysis,* Monograph Series, SPE, Richardson, TX (1977) **5.**
22. Matthews, C.S. and Russell, D.G.: *Pressure Buildup and Flow Tests in Wells,* Monograph Series, SPE, Richardson, TX (1967) **1.**
23. Wu, Y-S., Pruess, K., and Witherspoon, P.A.: "Displacement of a Newtonian Fluid by a Non-Newtonian Fluid in a Porous Medium," *Transport in Porous Media* (1991) **6,** 115–42.
24. Buckley, S.E. and Leverett, M.C.: "Mechanism of Fluid Displacement in Sands," *Trans.*, AIME (1942) **146,** 107–16.
25. Willhite, G.P.: *Waterflooding,* Textbook Series, SPE, Richardson, TX (1986) **3.**
26. Welge, H.J.: "Simplified Method for Computing Oil Recoveries by Gas or Water Drive," *Trans.*, AIME (1952) **195,** 91–98.
27. Pruess, K.: "Development of the General Purpose Simulator MULKOM," annual report, Earth Sciences Div., Lawrence Berkeley Laboratory, Berkeley, CA (1983).
28. Pruess, K.: "SHAFT, MULKOM, TOUGH: A Set of Numerical Simulators for Multiphase Fluid and Heat Flow," Report LBL-24430, Earth Sciences Div., Lawrence Berkeley Laboratory, Berkeley, CA (1988).
29. Narasimhan, T.N. and Witherspoon, P.A.: "An Integrated Finite Difference Method for Analyzing Fluid Flow in Porous Media," *Water Resources Research* (1976) **12,** No. 1, 57–64.
30. Duff, I.S.: "MA28—A Set of Fortran Subroutines for Sparse Unsymmetric Linear Equations," AERE Harwell, Oxfordshire, England, Report R 8730 (1977).
31. Pruess, K. and Wu, Y-S.: "On PVT-Data, Well Treatment, and Preparation of Input Data for an Isothermal Gas-Water-Foam Version of MULKOM," Report LBL-25783, UC-403, Earth Sciences Div., Lawrence Berkeley Laboratory, Berkeley, CA (1988).

Appendix—Numerical Model

The numerical simulations reported in this paper were performed with a modified and enhanced version of the general-purpose multiphase simulator MULKOM.[27,28] MULKOM uses an integral finite-difference method[29] to solve discretized mass-balance equations for n_c fluid components distributed among n_P phases. Time is discretized as a first-order finite difference, and all flow terms are formulated fully implicitly for numerical robustness and stability. Discretization results in a set of nonlinear algebraic equations that are solved by means of Newton-Raphson iteration. The linear algebra is performed with a sparse version of Gaussian elimination.[30] A more detailed description of the code is available in laboratory reports.[28,31]

The apparent viscosity functions for non-Newtonian fluids in porous media depend on the pore velocity, or the potential gradient, in a complex way. The rheological correlations for various non-Newtonian fluids are quite different. Therefore, it is impossible to develop a general numerical scheme that is universally applicable to all non-Newtonian fluids. Instead, a special treatment for a particular fluid of interest has to be worked out.

The flow of Bingham fluids is treated in the code by introducing an effective potential gradient, $\nabla\Phi_e$, whose scalar component in the flow direction, assumed to be the x direction, is defined as

$$(\nabla\Phi_e)_x = \begin{cases} (\nabla\Phi)_x - G & (\nabla\Phi)_x > G \\ (\nabla\Phi)_x + G & (\nabla\Phi)_x < -G \\ 0 & -G \le (\nabla\Phi)_x \le G \end{cases} \quad \ldots\ldots\ldots\ldots (A\text{-}1)$$

Darcy's law for a Bingham fluid is used in the code in the form

$$\vec{u} = -(k/\mu_B)\nabla\Phi_e \quad \ldots\ldots\ldots\ldots\ldots\ldots\ldots\ldots\ldots\ldots (A\text{-}2)$$

This treatment is much more efficient for simulation of Bingham-fluid flow in porous media than the direct use of a highly nonlinear apparent viscosity, as in Eq. 22a.

SI Metric Conversion Factors

bar	×	1.0*	E+05	= Pa
cp	×	1.0*	E−03	= Pa·s
ft	×	3.048*	E−01	= m
ft^2	×	9.290 304*	E−02	= m^2
lbm	×	4.535 924	E−01	= kg
lbm/gal	×	1.198 264	E+02	= kg/m^3
md	×	9.869 233	E−04	= μm^2
psi	×	6.894 757	E+00	= kPa
psi^{-1}	×	1.450 377	E−01	= kPa^{-1}

*Conversion factor is exact.

SPERE

Original SPE manuscript received for review April 4, 1990. Revised manuscript received Jan. 13, 1992. Paper accepted for publication April 10, 1992. Paper (SPE 20051) first presented at the 1990 SPE California Regional Meeting held in Ventura, April 4–6.